Published in final edited form as:
Cancer Cell. 2010 April 13; 17(4): 388–399. doi:10.1016/j.ccr.2010.02.027.

Itraconazole, a commonly used anti-fungal that inhibits Hedgehog pathway activity and cancer growth

James Kim[1], **Jean Y Tang**[2,9], **Ruoyu Gong**[4], **Jynho Kim**[1,4], **John J. Lee**[1], **Karl V. Clemons**[5,6], **Curtis R. Chong**[7,8], **Kris S. Chang**[9], **Mark Fereshteh**[10], **Tannishtha Reya**[10], **Jun O. Liu**[7,8], **Ervin H. Epstein**[9], **David A. Stevens**[5,6], and **Philip A. Beachy**[1,3,4,*]

[1]Department of Developmental Biology, Stanford University, Stanford, CA 94305, USA

[2]Department of Dermatology, Stanford University, Stanford, CA 94305, USA

[3]Institute for Stem Cell and Regenerative Medicine, Stanford University, Stanford, CA 94305, USA

[4]Howard Hughes Medical Institute, Stanford University, Stanford, CA 94305, USA

[5]Division of Infectious Diseases and Geographic Medicine, Stanford University, Stanford, CA 94305, USA

[6]California Institute for Medical Research, San Jose, CA 95128, USA

[7]Department of Pharmacology and Molecular Sciences, The Johns Hopkins University School of Medicine, Baltimore, Maryland 21205, USA

[8]The Johns Hopkins Clinical Compound Screening Initiative, The Johns Hopkins University School of Medicine, Baltimore, Maryland 21205, USA

[9]Children's Hospital Oakland Research Institute, Oakland, CA 94609, USA

[10]Department of Pharmacology and Cancer Biology, Duke University Medical Center, Durham, North Carolina 27710, USA

SUMMARY

In a screen of drugs previously tested in humans we identified itraconazole, a systemic antifungal, as a potent antagonist of the Hedgehog (Hh) signaling pathway that acts by a mechanism distinct from its inhibitory effect on fungal sterol biosynthesis. Systemically administered itraconazole, like other Hh pathway antagonists, can suppress Hh pathway activity and the growth of medulloblastoma in a mouse allograft model and does so at serum levels comparable to those in patients undergoing antifungal therapy. Mechanistically, itraconazole appears to act on the essential Hh pathway component Smoothened (Smo) by a mechanism distinct from that of

*Correspondence: pbeachy@stanford.edu.

cyclopamine and other known Smo antagonists, and prevents the ciliary accumulation of Smo normally caused by Hh stimulation.

INTRODUCTION

The Hh signaling pathway is critical for embryonic growth and patterning in organisms ranging from insects to mammals (Varjosalo and Taipale, 2008). Hh signaling also functions post-embryonically in tissue homeostasis through effects on stem or progenitor cells (Beachy et al., 2004). Inappropriate activity of the Hh signaling pathway also has been linked to tumor types that arise sporadically or in genetically predisposed individuals (Varjosalo and Taipale, 2008; Yauch et al., 2008).

Response to the Hh protein signal is governed by Patched (Ptch), a twelve pass transmembrane protein that restrains the activity of Smoothened (Smo), a member of the seven transmembrane family of serpentine receptors (Figure 1A). Hh protein, when present (Taipale and Beachy, 2001), binds Ptch and blocks its inhibition of Smo, thus permitting accumulation of Smo in the primary cilium (Corbit et al., 2005; Rohatgi et al., 2007), and causing activation of the Gli family of transcription factors. Pathway activation via Smo thus can occur either by Hh protein stimulation or through loss of Ptch activity, as seen in sporadic cancers or those that arise in the familial cancer predisposition syndrome, BCNS (Basal Cell Nevus Syndrome, associated with heterozygous mutation of the human *Ptch* gene).

Cyclopamine and other small molecules that antagonize Hh pathway activity (Chen et al., 2002a; Chen et al., 2002b; Cooper et al., 1998; Frank-Kamenetsky et al., 2002; Incardona et al., 1998; Taipale et al., 2000) have been found to act predominantly, although not exclusively, by binding the essential pathway component Smo. These small molecules have been effective in blocking Hh pathway-dependent growth of transformed cells, both *in vitro* (Taipale et al., 2000) and *in vivo* (Berman et al., 2002; Dierks et al., 2008; Romer et al., 2004; Yauch et al., 2008; Zhao et al., 2009), thus stimulating major efforts to develop small molecule antagonists of the Hh pathway as cancer therapeutics. However, drug development is time-consuming and costly (DiMasi et al., 2003; Frank, 2003), and we sought to circumvent this delay and expense by identifying Hh pathway antagonists among drugs that have been tested for toxicity in humans or even approved for human use by the FDA.

RESULTS AND DISCUSSION

We screened a library of ~2400 FDA-approved or post-phase I drugs (Chong et al., 2006a; Chong et al., 2006b) (now part of the Johns Hopkins Clinical Compound Library) for activity in inhibition of Hh signaling. This screen made use of a reporter cell line, Shh-Light2 (Taipale et al., 2000) (see Experimental Procedures), which contains a stably integrated Gli-luciferase reporter that responds to stimulation by ShhN, the active form of the Sonic hedgehog (Shh) signaling protein.

Although several dozen hits were identified from preliminary screening, only a few were active in pathway inhibition at concentrations achieved in humans. Among these the

microtubule inhibitors, including vinca alkaloids and their derivatives, consistently acted as Hh pathway antagonists (Figure S1). Their cytotoxic nature, however, precludes an extended and continuous course of treatment, as may be required for therapy of cancers by antagonism of Hh pathway activity (Berman et al., 2002; Romer et al., 2004; Yauch et al., 2008). A more promising candidate, itraconazole, was identified as a potent inhibitor of Hh pathway activity with an IC_{50} of approximately 800 nM (Figure 1B). This antifungal is commonly used in clinical practice as an orally delivered systemic treatment that can be sustained for months (Stevens, 2001).

Itraconazole inhibits 14-α-lanosterol demethylase (14LDM), by a mechanism in which the triazole group of itraconazole coordinates the heme Fe^{2+} in the cytochrome P-450 active site of 14LDM (Georgopapadakou and Walsh, 1996). 14LDM is critical for the biosynthesis of ergosterol in fungi and cholesterol in mammals (Lepesheva and Waterman, 2007) (Figure 1C). Itraconazole is significantly more potent in inhibiting the fungal enzyme (Lamb et al., 1999; Trosken et al., 2006) but has been shown to decrease human cholesterol levels at high doses (Schneider et al., 2007).To test whether azole antifungals in general act to inhibit Hh pathway activity we examined five other imidazole and triazole antifungal drugs. We found that itraconazole was by far the most potent inhibitor of Hh pathway activity, with an IC_{50} more than 10-fold lower than that of ketoconazole, its nearest rival ($IC_{50} \approx 9$ μM; see Figure 1D and Table S1). Hydroxy-itraconazole, the major metabolite of itraconazole in humans, is equally potent in its anti-fungal activity (Hostetler et al., 1993), and also inhibited Hh pathway activity ($IC_{50} \approx$ μM; see Figure 1E). Interestingly, fluconazole, a triazole like itraconazole with similar potency for 14LDM (Lamb et al., 1999; Trosken et al., 2006), shows no detectable inhibition of Hh pathway activity, even at a level 50-fold higher than the IC_{50} of itraconazole. We thus conclude that azole antifungal drugs as a general class are not inhibitors of Hh pathway activity.

The inability of fluconazole to inhibit Hh pathway activity, despite a similar potency for inhibition of 14LDM as itraconazole, suggests that the effect of itraconazole is not due to an effect on cellular cholesterol biosynthesis. Curiously, however, we noted that increasing serum levels in our assays blocked pathway inhibition by itraconazole (Figure 2A). This blocking effect was absent in lipid-depleted serum (Figure 2B), suggesting that a factor removed by lipid depletion of serum can interfere with or reverse the action of itraconazole. A similar interfering effect of serum but not lipiddepleted serum was noted with pathway activation by the small molecule agonist SAG (Chen et al., 2002b) (Figure S2A, B).

To investigate this serum effect further we directly tested the effects of cholesterol and its biosynthetic precursors lathosterol and desmosterol (see Figure 1C). In cultured cell signaling assays, our laboratory has shown that statins can inhibit Hh signal response, but only if transient cyclodextrin pretreatment is first used to deplete cellular sterols (Cooper et al., 2003); itraconazole in contrast does not require cyclodextrin pretreatment to inhibit the Hh pathway. Furthermore, although the addition of cholesterol to cyclodextrin pre-treated cultures in lipid-depleted serum reversed the inhibitory effects of statins on Hh response (Figure 2C) and cell proliferation (Figure S2C–E), the inhibitory effect of itraconazole was not reversed by supplementation of cultures with up to 25 μM of lathosterol or desmosterol (Figure 2D, E) or 250 μM cholesterol as an ethanolic solution or in water-soluble form

(Figure S2F, G). These results further reinforce the conclusion that itraconazole inhibition of Hh response is not mediated through inhibitory effects on sterol biosynthesis.

We next considered whether specific lipoprotein particles in serum might account for the reversal of itraconazole action on the Hh pathway, and found that LDL but not HDL or VLDL lipoprotein particles dramatically interfered with itraconazole action on Hh pathway activity (Figure 3A–C). The megalin member of the LDL receptor family (Fisher and Howie, 2006; Hussain et al., 1999), has been shown to bind and endocytose Shh (McCarthy et al., 2002), suggesting the possibility that LDL may interfere with itraconazole by affecting reception of the Hh signal. This is unlikely, however, as itraconazole acts below the level of the Hh receptor Ptch (see below); LDL furthermore interferes with itraconazole action even in cells lacking Ptch (Figure 3D). We thus conclude that the interfering effect of serum is not due to reversal of a sterol biosynthetic defect, nor through a LDL-mediated effect on Hh reception, but more likely through sequestration of itraconazole by LDL lipoprotein particles, which have been shown to sequester and interfere with the action of other hydrophobic compounds such as benzo(a)pyrene (Remsen and Shireman, 1981; Shu and Nichols, 1979) and *p*-dimethylaminoazobenzene (Chen et al., 1979).

We investigated the target of itraconazole action within the Hh pathway by examining cells with the *Ptch* gene disrupted by in frame fusion of *lacZ* (Goodrich et al., 1997; Taipale et al., 2000). Loss of Ptch function in these cells causes constitutive pathway activity and consequent expression of β-galactosidase through activation of the *Ptch* promoter. Itraconazole treatment of these cells inhibited β-galactosidase expression at levels similar to those required for inhibition of pathway activity in ShhN-stimulated Shh-Light2 cells ($IC_{50} \approx 900$ nM; Figure 4A). These results indicate that itraconazole acts independently of and downstream of Ptch. In contrast to *Ptch*−/− cells, the inhibitory action of itraconazole was bypassed by expression of SmoA1 (Taipale et al., 2000; Xie et al., 1998), a constitutively active oncogenic variant of murine Smo (Figure 4B), suggesting that itraconazole does not act downstream of Smo. To define further the target of itraconazole action, we combined itraconazole treatment with pathway activation by overexpression of Smo or by treatment with the oxysterols 20(*S*)- and 22(*S*)-hydroxycholesterol (Corcoran and Scott, 2006; Dwyer et al., 2007). We found that itraconazole blocked pathway activity produced by Smo overexpression (Figure 4C). Itraconazole also completely blocked oxysterol action ($IC_{50} \approx 270$ nM; Figure 4D), suggesting that oxysterols act on a target distinct from and upstream of the target of itraconazole.

The ability to suppress pathway activity from Smo overexpression but not from SmoA1 suggests that itraconazole may act by binding to Smo as an inverse agonist (Bond et al., 1995; Costa and Herz, 1989); binding to Smo also could account for itraconazole effects in *Ptch*−/− cells, or in cells treated with oxysterols. Therefore, we also examined the effect of itraconazole treatment on localization of Smo, which has been shown to accumulate in the primary cilium upon Hh stimulation (ref. (Corbit et al., 2005; Rohatgi et al., 2007); Figure 4E). We found that itraconazole treatment dramatically reduced Shh-induced accumulation of Smo in the primary cilium (Figure 3E), similar to other Smo antagonists, SANT-1 and SANT-2, but in contrast to cyclopamine which induced accumulation of Smo in the primary cilium (Rohatgi et al., 2009; Wang et al., 2009). The ability of itraconazole to suppress Shh-

induced accumulation of Smo in the primary cilium is consistent with direct action of itraconazole on Smo for pathway inactivation.

Like itraconazole, cyclopamine inhibits pathway activity in *Ptch−/−* cells (Taipale et al., 2000), in cells treated with oxysterols (Dwyer et al., 2007), and in cells overexpressing Smo (Taipale et al., 2000), but not in SmoA1-expressing cells (Taipale et al., 2000). As proposed above for itraconazole, cyclopamine and many other antagonists act by binding to Smo (Chen et al., 2002a; Chen et al., 2002b; Frank-Kamenetsky et al., 2002). We therefore tested itraconazole for Smo binding using BODIPY-cyclopamine, a fluorescent cyclopamine derivative, and a cell line that expresses Smo upon induction by treatment with tetracycline (Dwyer et al., 2007). We found that BODIPY-cyclopamine binding to Smo was not affected significantly by itraconazole, even at 10 μM, a concentration 12.5-fold higher than its IC_{50} (Figure 5A). This contrasts sharply with the potent cyclopamine derivative, KAAD-cyclopamine (IC_{50} = 20 nM), which reduced bound BODIPY-cyclopamine to near-background levels at 200 nM (Figure 5A).

Although itraconazole fails to compete with BODIPY-cyclopamine, it could nevertheless bind Smo at a distinct site from cyclopamine. If so, itraconazole conceivably could bind simultaneously with cyclopamine or with other small molecule agonists and antagonists that bind at the cyclopamine site. Itraconazole thus may synergize with cyclopamine or other Smo antagonists in pathway inhibition and it may act non-competitively with Smo agonists that bind at the cyclopamine site. Indeed, we found that the IC_{50} of KAAD-cyclopamine decreased from 20 nM to 2 nM with increasing doses of itraconazole (Figure 5B and Table S2), and that the IC_{50} of itraconazole decreases from 800 nM to 130 nM with increasing doses of KAAD-cyclopamine (Figure 5C and Table S3). In addition, the maximal degree of pathway activation by SAG, whose Smo binding site overlaps that of cyclopamine, was reduced by increasing concentrations of itraconazole without altering the SAG EC_{50} (Figure 5D and Table S4), indicating that itraconazole acts as a non-competitive inhibitor (Taylor and Insel, 1990). Itraconazole, in summary, behaves like an inverse agonist, suppresses the accumulation of Smo in the primary cilium, mutually enhances the potency of pathway inhibition in combination with cyclopamine, and acts as a non-competitive inhibitor of pathway activation by SAG. These characteristics of itraconazole are consistent with the binding of itraconazole to Smo at a distinct site from that of cyclopamine. As we have not demonstrated direct binding of itraconazole to Smo, however, the possibility remains that itraconazole may exert its inhibitory action on Smo through other indirect mechanisms.

Having characterized the Hh pathway inhibitory activity of itraconazole *in vitro*, we examined its effect *in vivo* by systemic treatment of animals subcutaneously engrafted with a primary medulloblastoma from a *Ptch+/−; p53−/−* mouse. Medulloblastomas from these mice depend on constitutive Hh pathway activity for their growth (Berman et al., 2002; Goodrich et al., 1997; Romer et al., 2004) and this growth can be inhibited by pathway antagonists (Berman et al., 2002; Romer et al., 2004). Treatment with itraconazole indeed inhibited growth of these subcutaneous allografts, with similar inhibition of tumor growth noted for animals treated with itraconazole at 100 mg/kg twice per day (b.i.d.) or 75 mg/kg b.i.d. (Figure 6A). Consistent with the synergistic effect of itraconazole and cyclopamine *in vitro*, combined treatment with itraconazole and cyclopamine produced an even greater

inhibition of tumor growth. Mice bearing control tumors were euthanized after 18 days as the tumors exceeded the size limits set forth by our Institutional Animal Care and Use Committee (IACUC).

At the end of the experiment, four hours after the last dose, we obtained serum and tumors from 3 mice in each treatment group. Itraconazole concentrations were measured using a bioassay method based on antifungal activity (Harvey et al., 1980; Hostetler et al., 1992; Rex et al., 1991) that does not distinguish between itraconazole and hydroxy-itraconazole (Hostetler et al., 1993). Itraconazole concentrations reported here therefore represent a combined measurement of itraconazole and hydroxy-itraconazole effects. Serum itraconazole concentrations were similar between the 100 mg/kg and 75 mg/kg groups (Figure 6B). Itraconazole levels achieved in tumors (Figure 6C) were similar to drug levels in serum, indicating that itraconazole has good tumor tissue penetration. The area-under-the curve (AUC) values for serum concentrations of itraconazole reached during a 24 hour pharmacokinetic study (Figure 6D) were also similar for itraconazole given at 100 mg/kg and 75 mg/kg (220 μg·hr/ml and 238 μg·hr/ml, respectively). These findings are consistent with previously published pharmacokinetic results (Hostetler et al., 1992).

We also tested the ability of itraconazole to inhibit pathway activity in tumor tissue in a separate experiment that made use of mice bearing secondary subcutaneous medulloblastoma allografts from the same original tumor as that used for studies of tumor growth (see above). These mice were treated either with 100 mg/kg itraconazole b.i.d. or 37.5 mg/kg cyclopamine b.i.d. The treated tumors showed decreased Gli1 mRNA levels, indicative of reduced Hh pathway activity as compared to cyclodextrin vehicle-treated controls (Figure 6E).

To further assess the activity of itraconazole on suppression of Hh-dependent tumors, we used *K14-CreER; Ptch+/−; p53 fl*/fl mice to generate endogenous basal cell carcinomas (BCC) of the skin (see Experimental Procedures). BCC tumors generated from these mice have increased levels of Hh pathway activity and their growth is suppressed by Hh pathway inhibitors (Xiao, 2009). Itraconazole treatment suppressed the growth of the endogenous BCC tumors when compared to the cyclodextrin vehicle control (Figure 7A). When itraconazole was stopped after 18 days of treatment (Figure 7A), the tumors began to grow again at a rate similar to that of vehicle-treated control tumors. At the end of the study, tumors from itraconazole-treated mice appeared to have greater levels of necrosis as compared to tumors from vehicle-treated mice, based on destruction of basophilic tumor cell nests and the eosinophilic stroma surrounding these nests (Figure 7B). Tabulation of necrosis scores, with a higher score indicating worse necrosis, confirmed that histologically-assessed necrosis was greater for itraconazole-treated BCC as compared to vehicle-treated tumors (Figure 7C).

The serum concentrations of itraconazole associated with an antitumor effect in our *in vivo* studies are higher than those reached in humans at regular therapeutic doses (Barone et al., 1993) (i.e.,400 mg/day orally for 15 days). Similar high serum levels of itraconazole (Sanchez et al., 1995), however, have been reported in patients treated for severe fungal infections. This high dose itraconazole therapy has ranged from 600 to 900 mg/day (Sanchez

et al., 1995; Sharkey et al., 1991; Takagi et al., 2001) over treatment periods ranging from 3 to 16 months, with occasional toxicities that were manageable (Sharkey et al., 1991). It is of interest that ketoconazole, another azole antifungal, has been used as second line therapy for androgen independent metastatic prostate cancer (Scholz et al., 2005; Trump et al., 1989) at doses 3–6 fold higher than its normal dose and with toxicities greater than those for high-dose itraconazole (Sugar et al., 1987). The use of ketoconazole in this context is believed to act by inhibiting androgen production, but we cannot rule out the possibility of an effect on Hh pathway activity.

Hh pathway activity has been characterized as contributing to growth of many tumor types (Varjosalo and Taipale, 2008; Yauch et al., 2008). Recent studies in the mouse have shown that another cancer, chronic myelogenous leukemia (CML), is dependent on Hh signaling. Smo activity is necessary for maintenance of CML stem cells and mouse and human CML that becomes resistant to tyrosine kinase inhibitor therapy remains sensitive to manipulation of Smo activity (Dierks et al., 2008; Zhao et al., 2009).

The importance of the Hh pathway in tumor growth has led to an active interest in the development of small molecule Hh pathway antagonists (Tremblay et al., 2009). Most of these molecules are either cyclopamine derivatives or they antagonize pathway by binding Smo at the same site as cyclopamine. Recent clinical tests of one of these cyclopamine mimics, GDC-0449 (Rudin et al., 2009; Von Hoff et al., 2009), produced promising results, suggesting that Hh pathway inhibition may represent an effective approach to cancer therapy. Further clinical testing will be required to establish efficacy and long term safety of such agents (Dlugosz and Talpaz, 2009).

Itraconazole has been studied for nearly 25 years, and we therefore have a good understanding of its safety and potential side effects. Furthermore, itraconazole is already used in human patients at doses that produce serum concentrations like those found to be effective in our murine medulloblastoma and BCC models. It is worth noting that itraconazole acts at a distinct site from cyclopamine; itraconazole and related compounds may therefore represent a helpful adjunct or alternative to the cyclopamine mimics currently under widespread development. For these reasons, particularly its well-known safety profile, it should be possible to quickly evaluate itraconazole either alone or in combination with other targeted therapies or cytotoxic agents in patients with tumors of known Hedgehog pathway dependence.

EXPERIMENTAL PROCEDURES

Cell culture assays for Hh pathway activation

Shh-Light2 cell line (Taipale et al., 2000) is a clonal NIH 3T3 cell line stably transfected with 8×-Gli1-binding site dependent firefly luciferase and *Renilla* luciferase reporters. SmoA1Light cell line is a clonal subline of Shh-Light cells stably transfected with oncogenic SmoA1 (Taipale et al., 2000). Shh-Light2 cells were maintained in DMEM media containing 10%(v/v) calf serum, penicillin, streptomycin, L-glutamine supplemented with Geneticin (Invitrogen) 400 μg/ml, and Zeocin (Invitrogen) 100 μg/ml. SmoA1Light cells were maintained DMEM media containing 10%(v/v) calf serum, penicillin, streptomycin, L-

glutamine supplemented with Geneticin (Invitrogen) 400 μg/ml and Hygromycin (CalBiochem) 100 μg/ml. *Ptch*−/− MEF cell line (Taipale et al., 2000) was maintained in DMEM media containing 10% fetal bovine serum (FBS), penicillin, streptomycin, L-glutamine supplemented with Geneticin 400 μg/ml.

ShhN conditioned medium (CM) was prepared as previously described (Maity et al., 2005). HEK 293 CM was used for control. HEK 293 CM was prepared in the same manner as ShhN CM. Stock ShhN CM and HEK 293 CM (for control) were diluted 10-fold with the appropriate media for various Hh pathway signaling assays.

For Smo overexpression assay in NIH-3T3 cells, Smo, GFP, Gli dependent firefly luciferase reporter, and TK-*Renilla* luciferase reporter vectors have been described previously (Taipale et al., 2000). Fugene 6 (Roche Applied Science) was used for transient transfection of the vectors at a ratio of 4 μl:1.5 μg (Fugene6:DNA). Each well of a 24 well multiwell plate was transfected with 375 ng of total DNA. Signaling assay for *Ptch*−/− cell performed similarly except for Fugene:DNA ratio of 3 μl:10 μg with 250 ng of total DNA per well of a 24 well plate.

All assays for Hh pathway activation were performed in 24 well tissue culture plates. Cells were grown in 10% (v/v) serum media until completely confluent. Drugs, 293 CM and ShhN CM were diluted in DMEM media containing 0.5% (v/v) serum unless otherwise noted in main text and figure legends. Cells were incubated for 40–46 hrs with drug treatments, except for the comparison of various azole (30 hours) and SmoA1 (30 hours) to minimize toxicity from the high concentrations of azole antifungals and forskolin, respectively. After internal normalization of firefly luciferase with tk-*Renilla* luciferase for each well, relative luciferase units were obtained by normalization of Hh pathway stimulated cells with unstimulated cells (all other conditions being equal) grown on a separate plate in parallel. All luminescence assays were performed on a Fluostar Optima (BMG Labtech). Luminescence assays were performed according to manufacturer's instructions using Dual Luciferase Assay Reporter System (Promega). β-Galactosidase activity of *Ptch*−/− cells were obtained using Galacto-Light Plus Reporter System (Applied Biosystems) per manufacturer's instructions. Total protein was obtained using BCA Protein Assay kit (Thermo Scientific) according to the manufacturer's instructions.

Dose response curves and IC_{50} values were determined by fitting the data with four parameter logarithmic nonlinear regression analysis using GraphPad Prism software.

Fluorescent BOPDIPY-cyclopamine Competition Assays

Maintenance and induction of Smo in the HEK 293S cell line stably expressing a tetracycline inducible Smo gene has been described previously (Dwyer et al., 2007). After two days of Smo induction, cells were incubated with BODIPY-cyclopamine 10 nM ± inhibitors at 37°C for 4–6 hours. Cells were trypsinized, washed with PBS after centrifugation, pelleted by centrifugation and resuspended in 0.5% calf serum/phenol red free DMEM. BODIPY fluorescence was measured on FACSAria (Becton Dickinson). FACS data was analyzed using FlowJo software.

Immunofluorescence

NIH-3T3 cells were grown to confluence on tissue culture treated glass cover slips (Fisher) and treated with various conditions for 6 hours as described previously for Hh pathway signaling assays. At the end of the incubation period, samples were fixed in methanol at −20°C and subsequently stained with appropriate antibodies. The antibodies used were as follows: rabbit polyclonal anti-Smo 1:750 dilution, mouse monoclonal anti-acetylated tubulin 1:1000 dilution (Sigma), AlexaFluor 488 goat anti-rabbit 1:667 dilution (Invitrogen), and AlexaFluor 594 goat anti-mouse 1:667 dilution (Invitrogen). Details of anti-Smo antibody have been described (Kim, 2009).

Microscopy

Images for ciliary accumulation of Smo were obtained on a Zeiss LSM 510 Meta Confocal microscope at the Stanford Institute for Neuro-Innovation & Translational Neuroscience. Maximum intensity overlay images of Z-stacks were obtained with Zeiss Zen software. Cilia from these images were quantified manually.

For presentation of images, representative 300 × 300 pixel portions of each metafile were cut and maximum intensity overlay images of Z-stack were produced using Zeiss Zen software. The cut images were enlarged using Adobe Photoshop software. For inset images, portions were cut and enlarged using Adobe Photoshop. Subsequently, red and green channels were offset using ImageJ software. All images were then recombined and brightened equally using Adobe Photoshop.

In vivo drug treatment studies

All mouse studies were approved by and conformed to the policies and regulations of the respective Institutional Animal Care and Use Committees at Stanford University and the Children's Hospital Oakland Research Institute.

Study of Medulloblastoma Tumor Growth Inhibition—Primary medulloblastoma from *Ptch+/−; p53−/−* mouse was dissected, minced and triturated through a 20 gauge needle under sterile conditions. Tumor was mixed in a 1:1 solution of PBS:growth factor reduced Matrigel (BD Bioscience) and equal volumes were allografted subcutaneously into right and left flanks of 6 to 7 wk old female outbred athymic nude mice (Charles River Laboratories, Wilmington, MA). Tumors were established with an average tumor volume of each arm ~110 mm^3 before treatment. Tumors were measured with vernier calipers every 3–4 days and tumor volume (Berman et al., 2002) was calculated as (width × length × ([0.5× (length+width)]). Drinking water was acidified. Animals were treated twice per day, 10–14 hours apart by oral gavage with equal volumes of 40% (w/v) 2-hydroxypropyl-β-cyclodextrin (HPCD) solution as control and drugs. Oral itraconazole solution 10 mg/ml (Ortho-Biotec) was used for itraconazole 100 mg/kg arm. Oral itraconazole solution contains 40% (w/v) HPCD to solubilize itraconazole (Martin, 1999). For itraconazole 75 mg/kg arm, oral itraconazole solution was diluted to 7.5 mg/ml with sterile water. Cyclopamine was dissolved in 10% (w/v) HPCD/0.1 M sodium citrate/phosphate solution (pH 3) (Feldmann et al., 2007) at a concentration of 3.75 mg/ml. For itraconazole 100 mg/kg-cyclopamine 25 mg/kg, cyclopamine powder was dissolved in oral itraconazole 10

mg/ml solution to a final concentration of 2.5 mg/ml. A one way ANOVA was used to compare all treatment arms using GraphPad Prism software.

Study of Treatment for Hh Pathway Inhibition—An untreated primary medulloblastoma allograft from the tumor growth study was minced, digested into a single cell suspension with collagenase IV (Worthington Biochemical), aliquoted and stored in liquid nitrogen. Medulloblastoma cells were thawed and incubated overnight in defined serum free media (Kalani et al., 2008) containing B-27 supplement without vitamin A(Invitrogen), mouse EGF 20 ng/ml (Peprotech), mouse bFGF 20 ng/ml (Invitrogen), minimal non-essential amino acids (Invitrogen), N-acetyl cysteine 60 μg/ml, Glutamax (Invitrogen) in Neurobasal A medium (Invitrogen). Cells were pelleted, washed with PBS, and mixed in 1:1 solution of PBS:growth factor reduced Matrigel as noted above. Approximately 1.2 million cells were injected into the flank of nude mice as noted above. Tumors were established and mice were treated twice per day by oral gavage for four days. Drugs were prepared as noted above.

Generation of Endogenous Basal Cell Carcinoma—Different mice carrying the *K14-Cre-ER* transgene (Metzger et al., 2005), the *floxed p53* allele (Jonkers et al., 2001) and the *Ptch1+/−* (Goodrich et al., 1997) alleles were bred together to generate *Ptch1+/−; K14-Cre-ER; p53fl/fl* mice. We treated these mice at age 6 weeks with 100 μg/day of tamoxifen administered intraperitoneally for three consecutive days. At 8 weeks of age, *Ptch1+/− K14-Cre-ER p53fl/fl* mice were exposed to 4 Gy of ionizing radiation (IR). Mice develop visible BCC tumors at 6 months of age.

Study of BCC Tumor Growth Inhibition—Four mice with a total of 20 visible BCC tumors were gavaged twice daily with oral itraconazole solution (Ortho-Biotec) 100mg/kg, for 18 days. Itraconazole was discontinued on day 19, two mice were euthanized on day 19 and the tumors dissected for further examination and BCC tumors of the two remaining were followed until 22 days. Two mice with 10 BCC tumors were treated with 40% w/v HPCD (Sigma) for an average of 22 days at which point the mice were euthanized because of their large tumor size that exceeded our animal care guidelines. We measured the change in the long axis of BCC tumor size with calipers every 3 days (So et al., 2004). Pair-wise comparisons between cyclodextrin control and itraconazole treatment arms were done using a two-sided unpaired *t*-test with GraphPad Prism software.

Necrosis Scoring of BCC tumors

H&E sections of paraffin embedded BCC tumors after the growth inhibition study were examined for necrosis. Necrosis was scored as follows: 0 = No evidence of necrosis with large basaloid cells; 1 = mild necrosis with nuclear pyknosis; 2 = moderate necrosis with <25% necrosis; 3 = severe necrosis with > 25% necrosis. After tabulation of necrosis scores, pair-wise comparison between cyclodextrin control and itraconazole treatment tumors were made using a two-sided unpaired *t*-test with GraphPad Prism software.

Itraconazole levels

For the itraconazole pharmacokinetic study, 7–8 week old female outbred athymic nude mice (Charles River Laboratories, Wilmington, MA) were given one dose of itraconazole 100 mg/kg or 75 mg/kg or equivolume of 40% HPCD solution at time = 0 hr point. At each time point, three mice from each treatment arm were anesthetized, exsanguinated, blood collected and euthanized. Blood was allowed to clot and the resultant serum used for bioassays to measure itraconazole levels. Serum from untreated athymic nude mice was used for obtaining the standard curve for the bioassays. Area under the curve (AUC) from 0 – 24 hours were calculated using GraphPad Prism software with the trapezoidal rule method.

For itraconazole concentrations from the medulloblastoma allograft study, serum from three mice of each treatment and control arm were obtained at the end of the study in a similar manner to the pharmacokinetic study.

For itraconazole concentrations of tumors from the medulloblastoma allograft study, mice were exsanguinated under isoflurane anesthesia and perfused with PBS via the left ventricle to remove any blood which might confound tumor itraconazole levels. Tumors were excised and frozen on dry ice, ground, and extracted with solvent for drug assay as previously described (Clemons et al., 2002). Serum and tissue antifungal itraconazole concentrations were determined by bioassay method, with itraconazole standards, as described (Clemons et al., 2002; Harvey et al., 1980; Hostetler et al., 1992; Rex et al., 1991).

Supplementary Material

Refer to Web version on PubMed Central for supplementary material.

Acknowledgments

We thank N. Sever for providing HEK 293S inducible Smo cell line, M. Martinez, and A.J. Tong for technical assistance, P. Lovelace for assistance with FACS, A. Olson for assistance with confocal microscopy, and M. Scott for helpful comments and discussion of the manuscript. J.K. is a recipient of the American Society of Clinical Oncology Young Investigator Award. This research was supported in part by grants from the Prostate Cancer Foundation, from the Stanford University Center for Children’s Brain Tumors, and from the National Institutes of Health. P.A.B is an investigator of the Howard Hughes Medical Institute.

REFERENCES

Barone JA, Koh JG, Bierman RH, Colaizzi JL, Swanson KA, Gaffar MC, Moskovitz BL, Mechlinski W, Van de Velde V. Food interaction and steady-state pharmacokinetics of itraconazole capsules in healthy male volunteers. Antimicrob Agents Chemother. 1993; 37:778–784. [PubMed: 8388198]

Beachy PA, Karhadkar SS, Berman DM. Tissue repair and stem cell renewal in carcinogenesis. Nature. 2004; 432:324–331. [PubMed: 15549094]

Berman DM, Karhadkar SS, Hallahan AR, Pritchard JI, Eberhart CG, Watkins DN, Chen JK, Cooper MK, Taipale J, Olson JM, Beachy PA. Medulloblastoma growth inhibition by hedgehog pathway blockade. Science. 2002; 297:1559–1561. [PubMed: 12202832]

Bond RA, Leff P, Johnson TD, Milano CA, Rockman HA, McMinn TR, Apparsundaram S, Hyek MF, Kenakin TP, Allen LF, et al. Physiological effects of inverse agonists in transgenic mice with myocardial overexpression of the beta 2-adrenoceptor. Nature. 1995; 374:272–276. [PubMed: 7885448]

Chen JK, Taipale J, Cooper MK, Beachy PA. Inhibition of Hedgehog signaling by direct binding of cyclopamine to Smoothened. Genes Dev. 2002a; 16:2743–2748. [PubMed: 12414725]

Chen JK, Taipale J, Young KE, Maiti T, Beachy PA. Small molecule modulation of Smoothened activity. Proc Natl Acad Sci U S A. 2002b; 99:14071–14076. [PubMed: 12391318]

Chen TC, Bradley WA, Gotto AM Jr, Morrisett JD. Binding of the chemical carcinogen, p-dimethylaminoazobenzene, by human plasma low density lipoproteins. FEBS Lett. 1979; 104:236–240. [PubMed: 225207]

Chong CR, Chen X, Shi L, Liu JO, Sullivan DJ Jr. A clinical drug library screen identifies astemizole as an antimalarial agent. Nat Chem Biol. 2006a; 2:415–416. [PubMed: 16816845]

Chong CR, Qian DZ, Pan F, Wei Y, Pili R, Sullivan DJ Jr, Liu JO. Identification of type 1 inosine monophosphate dehydrogenase as an antiangiogenic drug target. J Med Chem. 2006b; 49:2677–2680. [PubMed: 16640327]

Clemons KV, Sobel RA, Williams PL, Pappagianis D, Stevens DA. Efficacy of intravenous liposomal amphotericin B (AmBisome) against coccidioidal meningitis in rabbits. Antimicrob Agents Chemother. 2002; 46:2420–2426. [PubMed: 12121913]

Cooper MK, Porter JA, Young KE, Beachy PA. Teratogen-mediated inhibition of target tissue response to Shh signaling. Science. 1998; 280:1603–1607. [PubMed: 9616123]

Cooper MK, Wassif CA, Krakowiak PA, Taipale J, Gong R, Kelley RI, Porter FD, Beachy PA. A defective response to Hedgehog signaling in disorders of cholesterol biosynthesis. Nat Genet. 2003; 33:508–513. [PubMed: 12652302]

Corbit KC, Aanstad P, Singla V, Norman AR, Stainier DY, Reiter JF. Vertebrate Smoothened functions at the primary cilium. Nature. 2005; 437:1018–1021. [PubMed: 16136078]

Corcoran RB, Scott MP. Oxysterols stimulate Sonic hedgehog signal transduction and proliferation of medulloblastoma cells. Proc Natl Acad Sci U S A. 2006; 103:8408–8413. [PubMed: 16707575]

Costa T, Herz A. Antagonists with negative intrinsic activity at delta opioid receptors coupled to GTP-binding proteins. Proc Natl Acad Sci U S A. 1989; 86:7321–7325. [PubMed: 2552439]

Dierks C, Beigi R, Guo GR, Zirlik K, Stegert MR, Manley P, Trussell C, Schmitt-Graeff A, Landwerlin K, Veelken H, Warmuth M. Expansion of Bcr-Abl-positive leukemic stem cells is dependent on Hedgehog pathway activation. Cancer Cell. 2008; 14:238–249. [PubMed: 18772113]

DiMasi JA, Hansen RW, Grabowski HG. The price of innovation: new estimates of drug development costs. J Health Econ. 2003; 22:151–185. [PubMed: 12606142]

Dlugosz AA, Talpaz M. Following the hedgehog to new cancer therapies. N Engl J Med. 2009; 361:1202–1205. [PubMed: 19726764]

Dwyer JR, Sever N, Carlson M, Nelson SF, Beachy PA, Parhami F. Oxysterols are novel activators of the hedgehog signaling pathway in pluripotent mesenchymal cells. J Biol Chem. 2007; 282:8959–8968. [PubMed: 17200122]

Feldmann G, Dhara S, Fendrich V, Bedja D, Beaty R, Mullendore M, Karikari C, Alvarez H, Iacobuzio-Donahue C, Jimeno A, et al. Blockade of hedgehog signaling inhibits pancreatic cancer invasion and metastases: a new paradigm for combination therapy in solid cancers. Cancer Res. 2007; 67:2187–2196. [PubMed: 17332349]

Fisher CE, Howie SE. The role of megalin (LRP-2/Gp330) during development. Dev Biol. 2006; 296:279–297. [PubMed: 16828734]

Frank RG. New estimates of drug development costs. J Health Econ. 2003; 22:325–330. [PubMed: 12606149]

Frank-Kamenetsky M, Zhang XM, Bottega S, Guicherit O, Wichterle H, Dudek H, Bumcrot D, Wang FY, Jones S, Shulok J, et al. Small-molecule modulators of Hedgehog signaling: identification and characterization of Smoothened agonists and antagonists. J Biol. 2002; 1:10. [PubMed: 12437772]

Georgopapadakou NH, Walsh TJ. Antifungal agents: chemotherapeutic targets and immunologic strategies. Antimicrob Agents Chemother. 1996; 40:279–291. [PubMed: 8834867]

Goodrich LV, Milenkovic L, Higgins KM, Scott MP. Altered neural cell fates and medulloblastoma in mouse patched mutants. Science. 1997; 277:1109–1113. [PubMed: 9262482]

Harvey RP, Isenberg RA, Stevens DA. Molecular modifications of imidazole compounds: Studies of activity and synergy in vitro and of pharmacology and therapy of blastomycosis in a mouse model. Rev Infect Dis. 1980; 2:559–569.

Hostetler JS, Hanson LH, Stevens DA. Effect of cyclodextrin on the pharmacology of antifungal oral azoles. Antimicrob Agents Chemother. 1992; 36:477–480. [PubMed: 1605615]

Hostetler JS, Heykants J, Clemons KV, Woestenborghs R, Hanson LH, Stevens DA. Discrepancies in bioassay and chromatography determinations explained by metabolism of itraconazole to hydroxyitraconazole: studies of interpatient variations in concentrations. Antimicrob Agents Chemother. 1993; 37:2224–2227. [PubMed: 8257148]

Hussain MM, Strickland DK, Bakillah A. The mammalian low-density lipoprotein receptor family. Annu Rev Nutr. 1999; 19:141–172. [PubMed: 10448520]

Incardona JP, Gaffield W, Kapur RP, Roelink H. The teratogenic Veratrum alkaloid cyclopamine inhibits sonic hedgehog signal transduction. Development. 1998; 125:3553–3562. [PubMed: 9716521]

Jonkers J, Meuwissen R, van der Gulden H, Peterse H, van der Valk M, Berns A. Synergistic tumor suppressor activity of BRCA2 and p53 in a conditional mouse model for breast cancer. Nat Genet. 2001; 29:418–425. [PubMed: 11694875]

Kalani MY, Cheshier SH, Cord BJ, Bababeygy SR, Vogel H, Weissman IL, Palmer TD, Nusse R. Wnt-mediated self-renewal of neural stem/progenitor cells. Proc Natl Acad Sci U S A. 2008; 105:16970–16975. [PubMed: 18957545]

Kim J, Kato M, Beachy PA. Gli2 Trafficking links Hedgehog-dependent activation of Smoothened in the primary cilium to transcriptional activation in the nucleus. Proc Natl Acad Sci U S A. 2009

Lamb DC, Kelly DE, Waterman MR, Stromstedt M, Rozman D, Kelly SL. Characteristics of the heterologously expressed human lanosterol 14alpha-demethylase (other names: P45014DM, CYP51, P45051) and inhibition of the purified human and Candida albicans CYP51 with azole antifungal agents. Yeast. 1999; 15:755–763. [PubMed: 10398344]

Lepesheva GI, Waterman MR. Sterol 14alpha-demethylase cytochrome P450 (CYP51), a P450 in all biological kingdoms. Biochim Biophys Acta. 2007; 1770:467–477. [PubMed: 16963187]

Maity T, Fuse N, Beachy PA. Molecular mechanisms of Sonic hedgehog mutant effects in holoprosencephaly. Proc Natl Acad Sci U S A. 2005; 102:17026–17031. [PubMed: 16282375]

Martin MV. The use of fluconazole and itraconazole in the treatment of Candida albicans infections: a review. J Antimicrob Chemother. 1999; 44:429–437. [PubMed: 10588302]

McCarthy RA, Barth JL, Chintalapudi MR, Knaak C, Argraves WS. Megalin functions as an endocytic sonic hedgehog receptor. J Biol Chem. 2002; 277:25660–25667. [PubMed: 11964399]

Metzger D, Li M, Chambon P. Targeted somatic mutagenesis in the mouse epidermis. Methods Mol Biol. 2005; 289:329–340. [PubMed: 15502196]

Remsen JF, Shireman RB. Effect of low-density lipoprotein on the incorporation of benzo(a)pyrene by cultured cells. Cancer Res. 1981; 41:3179–3185. [PubMed: 6265078]

Rex JH, Hanson LH, Amantea MA, Stevens DA, Bennett JE. Standardization of a fluconazole bioassay and correlation of results with those obtained by high-pressure liquid chromatography. Antimicrob Agents Chemother. 1991; 35:846–850. [PubMed: 1854166]

Rohatgi R, Milenkovic L, Corcoran RB, Scott MP. Hedgehog signal transduction by Smoothened: pharmacologic evidence for a 2-step activation process. Proc Natl Acad Sci U S A. 2009; 106:3196–3201. [PubMed: 19218434]

Rohatgi R, Milenkovic L, Scott MP. Patched1 regulates hedgehog signaling at the primary cilium. Science. 2007; 317:372–376. [PubMed: 17641202]

Romer JT, Kimura H, Magdaleno S, Sasai K, Fuller C, Baines H, Connelly M, Stewart CF, Gould S, Rubin LL, Curran T. Suppression of the Shh pathway using a small molecule inhibitor eliminates medulloblastoma in Ptc1(+/−)p53(−/−) mice. Cancer Cell. 2004; 6:229–240. [PubMed: 15380514]

Rudin CM, Hann CL, Laterra J, Yauch RL, Callahan CA, Fu L, Holcomb T, Stinson J, Gould SE, Coleman B, et al. Treatment of medulloblastoma with hedgehog pathway inhibitor GDC-0449. N Engl J Med. 2009; 361:1173–1178. [PubMed: 19726761]

Sanchez C, Mauri E, Dalmau D, Quintana S, Aparicio A, Garau J. Treatment of cerebral aspergillosis with itraconazole: do high doses improve the prognosis? Clin Infect Dis. 1995; 21:1485–1487. [PubMed: 8749640]

Schneider B, Gerdsen R, Plat J, Dullens S, Bjorkhem I, Diczfalusy U, Neuvonen PJ, Bieber T, von Bergmann K, Lutjohann D. Effects of high-dose itraconazole treatment on lipoproteins in men. Int J Clin Pharmacol Ther. 2007; 45:377–384. [PubMed: 17725244]

Scholz M, Jennrich R, Strum S, Brosman S, Johnson H, Lam R. Long-term outcome for men with androgen independent prostate cancer treated with ketoconazole and hydrocortisone. J Urol. 2005; 173:1947–1952. [PubMed: 15879788]

Sharkey PK, Rinaldi MG, Dunn JF, Hardin TC, Fetchick RJ, Graybill JR. High-dose itraconazole in the treatment of severe mycoses. Antimicrob Agents Chemother. 1991; 35:707–713. [PubMed: 1648887]

Shu HP, Nichols AV. Benzo(a)pyrene uptake by human plasma lipoproteins in vitro. Cancer Res. 1979; 39:1224–1230. [PubMed: 217532]

So PL, Lee K, Hebert J, Walker P, Lu Y, Hwang J, Kopelovich L, Athar M, Bickers D, Aszterbaum M, Epstein EH Jr. Topical tazarotene chemoprevention reduces Basal cell carcinoma number and size in Ptch1+/− mice exposed to ultraviolet or ionizing radiation. Cancer Res. 2004; 64:4385–4389. [PubMed: 15231643]

Stevens, DAe. Managing Fungal Infections in the 21st Century: Focus on Itraconazole. Drugs. 2001; 61:1–56.

Sugar AM, Alsip SG, Galgiani JN, Graybill JR, Dismukes WE, Cloud GA, Craven PC, Stevens DA. Pharmacology and toxicity of high-dose ketoconazole. Antimicrob Agents Chemother. 1987; 31:1874–1878. [PubMed: 3326525]

Taipale J, Beachy PA. The Hedgehog and Wnt signalling pathways in cancer. Nature. 2001; 411:349–354. [PubMed: 11357142]

Taipale J, Chen JK, Cooper MK, Wang B, Mann RK, Milenkovic L, Scott MP, Beachy PA. Effects of oncogenic mutations in Smoothened and Patched can be reversed by cyclopamine. Nature. 2000; 406:1005–1009. [PubMed: 10984056]

Takagi K, Yoshida A, Yamauchi T, Yamashita T, Iwasaki H, Tsutani H, Maezawa Y, Baba H, Ueda T. Successful treatment of Aspergillus spondylodiscitis with high-dose itraconazole in a patient with acute myelogenous leukemia. Leukemia. 2001; 15:1670–1671. [PubMed: 11587231]

Taylor, P.; Insel, PA. Quantitation of Pharmacologic Antagonism. In: Pratt, WP.; Taylor, P., editors. Principles of Drug Action: The Basis of Pharmacology. New York City: Churchill Livingstone; 1990. p. 61-66.

Tremblay MR, Nesler M, Weatherhead R, Castro AC. Recent patents for Hedgehog pathway inhibitors for the treatment of malignancy. Expert Opin Ther Pat. 2009; 19:1039–1056. [PubMed: 19505195]

Trosken ER, Adamska M, Arand M, Zarn JA, Patten C, Volkel W, Lutz WK. Comparison of lanosterol-14 alpha-demethylase (CYP51) of human and Candida albicans for inhibition by different antifungal azoles. Toxicology. 2006; 228:24–32. [PubMed: 16989930]

Trump DL, Havlin KH, Messing EM, Cummings KB, Lange PH, Jordan VC. High-dose ketoconazole in advanced hormone-refractory prostate cancer: endocrinologic and clinical effects. J Clin Oncol. 1989; 7:1093–1098. [PubMed: 2474059]

Varjosalo M, Taipale J. Hedgehog: functions and mechanisms. Genes Dev. 2008; 22:2454–2472. [PubMed: 18794343]

Von Hoff DD, LoRusso PM, Rudin CM, Reddy JC, Yauch RL, Tibes R, Weiss GJ, Borad MJ, Hann CL, Brahmer JR, et al. Inhibition of the hedgehog pathway in advanced basal-cell carcinoma. N Engl J Med. 2009; 361:1164–1172. [PubMed: 19726763]

Wang Y, Zhou Z, Walsh CT, McMahon AP. Selective translocation of intracellular Smoothened to the primary cilium in response to Hedgehog pathway modulation. Proc Natl Acad Sci U S A. 2009; 106:2623–2628. [PubMed: 19196978]

Xiao TZ, Tang JY, Wu A, Shpall E, Khaimsky I, So P, Epstein EH Jr. Hedgehog signaling of BCC is inhibited by Vitamin D: Implication for a chemopreventive agent against BCC carcinogenesis. J Invest Dermatol. 2009; 129:S32.

Xie J, Murone M, Luoh SM, Ryan A, Gu Q, Zhang C, Bonifas JM, Lam CW, Hynes M, Goddard A, et al. Activating Smoothened mutations in sporadic basal-cell carcinoma. Nature. 1998; 391:90–92. [PubMed: 9422511]

Yauch RL, Gould SE, Scales SJ, Tang T, Tian H, Ahn CP, Marshall D, Fu L, Januario T, Kallop D, et al. A paracrine requirement for hedgehog signalling in cancer. Nature. 2008

Zhao C, Chen A, Jamieson CH, Fereshteh M, Abrahamsson A, Blum J, Kwon HY, Kim J, Chute JP, Rizzieri D, et al. Hedgehog signalling is essential for maintenance of cancer stem cells in myeloid leukaemia. Nature. 2009; 458:776–779. [PubMed: 19169242]

SIGNIFICANCE

The inappropriate activity of the Hh signaling pathway noted in a variety of tumor types has prompted efforts to develop small molecule antagonists of Hh pathway signaling. Such drug development efforts, however, are costly and time-consuming. With the identification of itraconazole, a commonly used systemic antifungal, as a potent inhibitor of the Hh pathway *in vitro* and *in vivo*, it may be possible to avoid some of the expense and delay associated with de novo development of Hh pathway antagonists. Supporting the rapid entry of itraconazole into clinical trials in the treatment of Hh-dependent cancers, serum levels that inhibit growth of tumors in mice are comparable to those reported in humans.

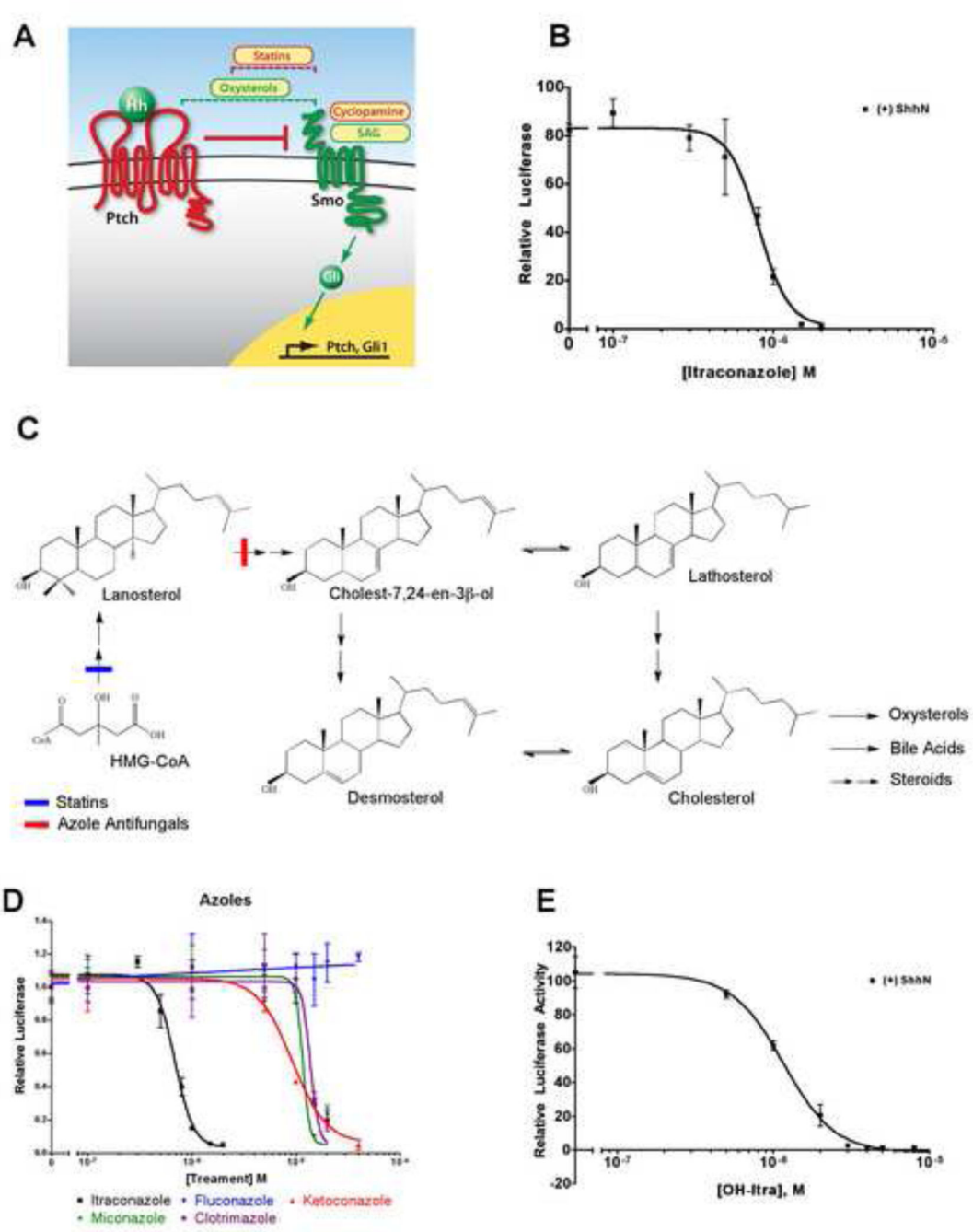

Figure 1. Itraconazole inhibits Hh signaling

(A) A schematic view of the Hedgehog (Hh) signaling pathway. In the absence of Hh, Patched (Ptch) suppresses Smoothened (Smo) function. Hh, when present, binds to and inhibits Ptch, permitting Smo accumulation in the primary cilium (not shown) and causing activation of the pathway via the Gli family of transcription factors. *Ptch* and *Gli1* are themselves transcriptional targets of the pathway. Oxysterols (dashed green bracket) act between Ptch and Smo, as pathway activators, whereas statins (dashed red bracket) act downstream of Ptch and at or upstream of Smo, as pathway inhibitors. SAG and

cyclopamine activate and inhibit the pathway, respectively, by binding to the transmembrane domain of Smo. Activators and inhibitors of the pathway are labeled in green and red, respectively. (B) Hh signaling assays. Luciferase reporter activity under the control of an 8×-Gli binding site in the Shh-Light2 reporter cell line was measured upon stimulation with ShhN-containing medium. Itraconazole blocked Hh pathway activity (IC_{50}≈800 nM). (C) Schematic view of mammalian cholesterol biosynthesis from 3-hydroxy-3-methyl-glutaryl-CoA (HMG-CoA). Statins inhibit HMG-CoA reductase whereas azole antifungal drugs inhibit 14α-lanosterol demethylase (14LDM), as indicated. Lathosterol and desmosterol are cholesterol precursors downstream of 14LDM. (D) Among the azole antifungals, itraconazole was the most potent inhibitor of Hh pathway activity. (E) Hydroxy-itraconazole, the major metabolite of itraconazole in mammals, also inhibited the Hh pathway (IC_{50} ≈1.2 μM). All signaling assays were performed with Shh-Light2 cells in 0.5% serum media and data are shown as the mean of triplicates ± s.d.
See also Figure S1 and Table S1.

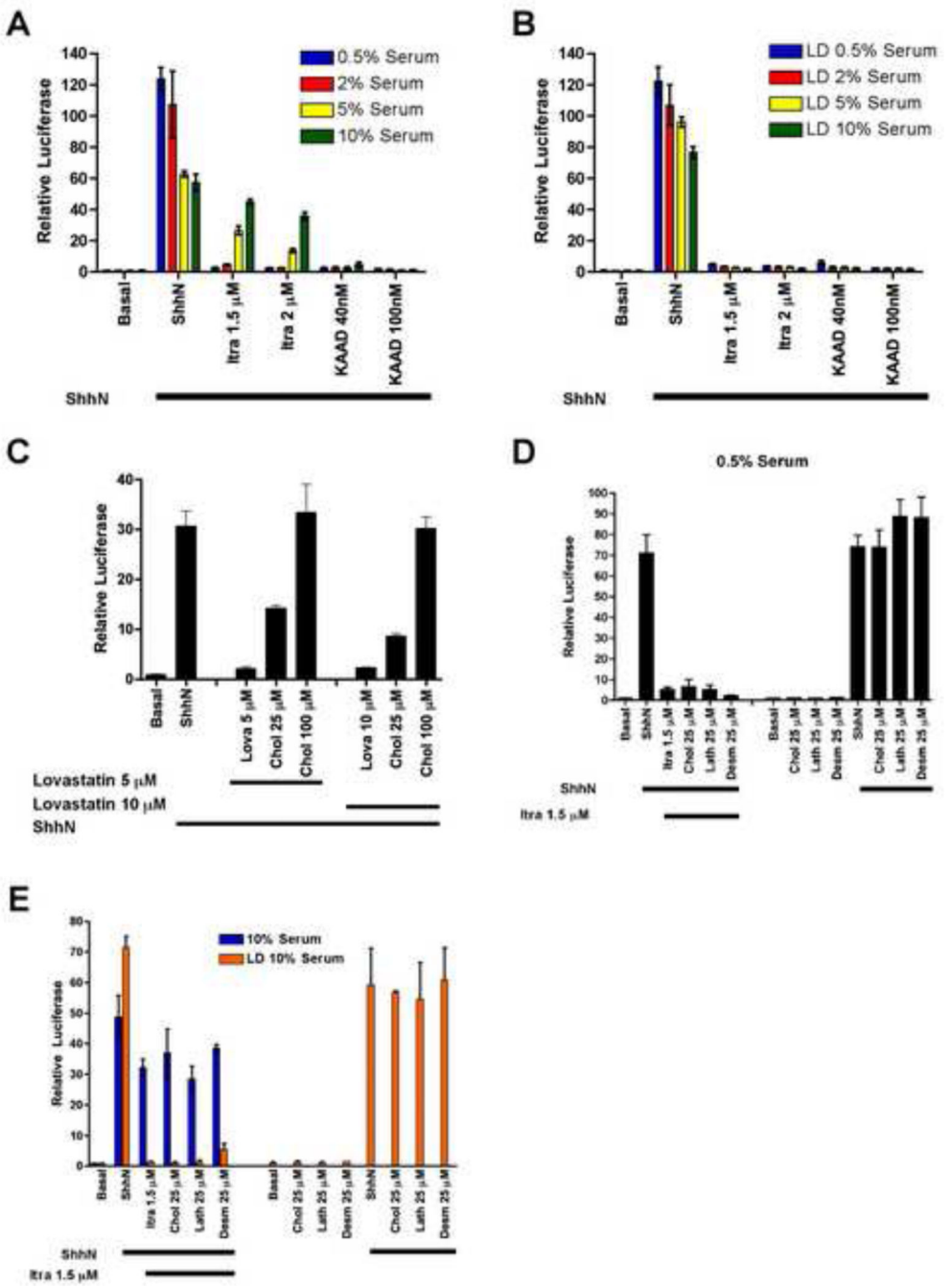

Figure 2. Inhibition of Hh signaling by itraconazole is not mediated by effects on cholesterol biosynthesis

(A) Increasing serum concentrations attenuated the inhibitory activity of itraconazole but not KAAD-cyclopamine. (B) The attenuating effect of serum was abolished by lipid depletion (LD). (C) Shh-Light2 cells were pretreated with methyl-β-cyclodextrin (MβCD) 8 mM in DMEM for 45 minutes to remove sterols from the cell surface (Cooper et al., 2003). Lovastatin, an HMG-CoA reductase inhibitor, inhibited Hh pathway activity induced by ShhN. Cholesterol, in ethanol solution, reversed the pathway inhibition due to lovastatin (D, E) Lathosterol, desmosterol, and cholesterol failed to rescue Hh pathway inhibition by

itraconazole under low (D) or lipid depleted (E) serum conditions. All signaling assays were performed with Shh-Light2 cells and data are mean of triplicates ± s.d.
See also Figure S2.

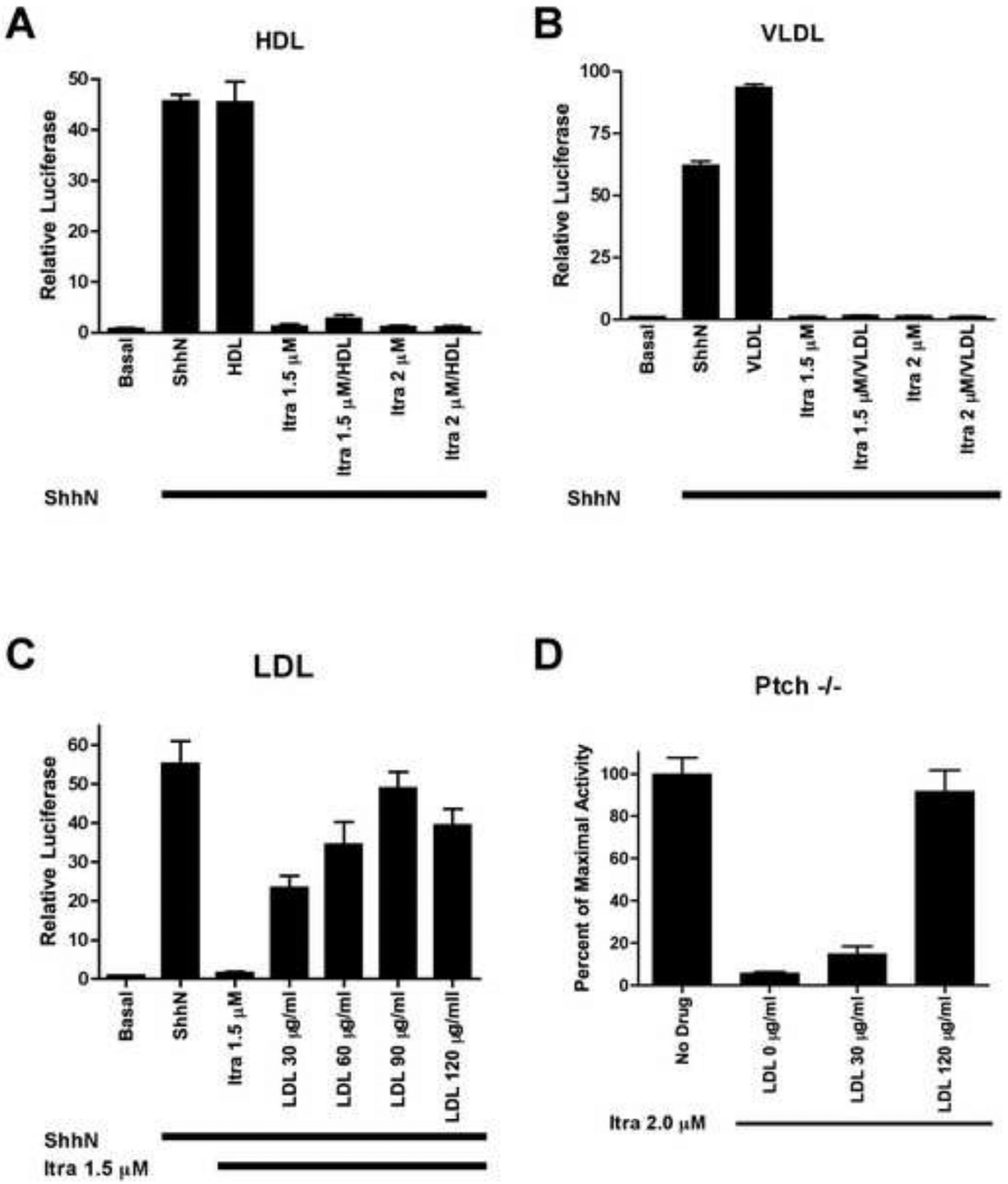

Figure 3. Low density lipoprotein modulate the Hh pathway inhibitory effects of itraconazole

(A) High density lipoprotein (HDL) 100 μg/ml and (B) very low density lipoprotein (VLDL) 6.5 μg/ml cannot reverse Hh pathway inhibition by itraconazole. (C, D) Titration of low density lipoprotein (LDL) up to 120 μg/ml rescues either induced Hh pathway activity by ShhN ligand in Shh-Light2 cells (C) or constitutively active pathway in *Ptch*−/− cells (Goodrich et al., 1997; Taipale et al., 2000) (D) from the inhibitory effects of itraconazole. All signaling assays were performed in lipid depleted 10% calf serum media for Shh-Light2

cells (A–C) and 0.5% fetal bovine serum media for *Ptch*−/− cells. Data are mean of triplicates ± s.d.

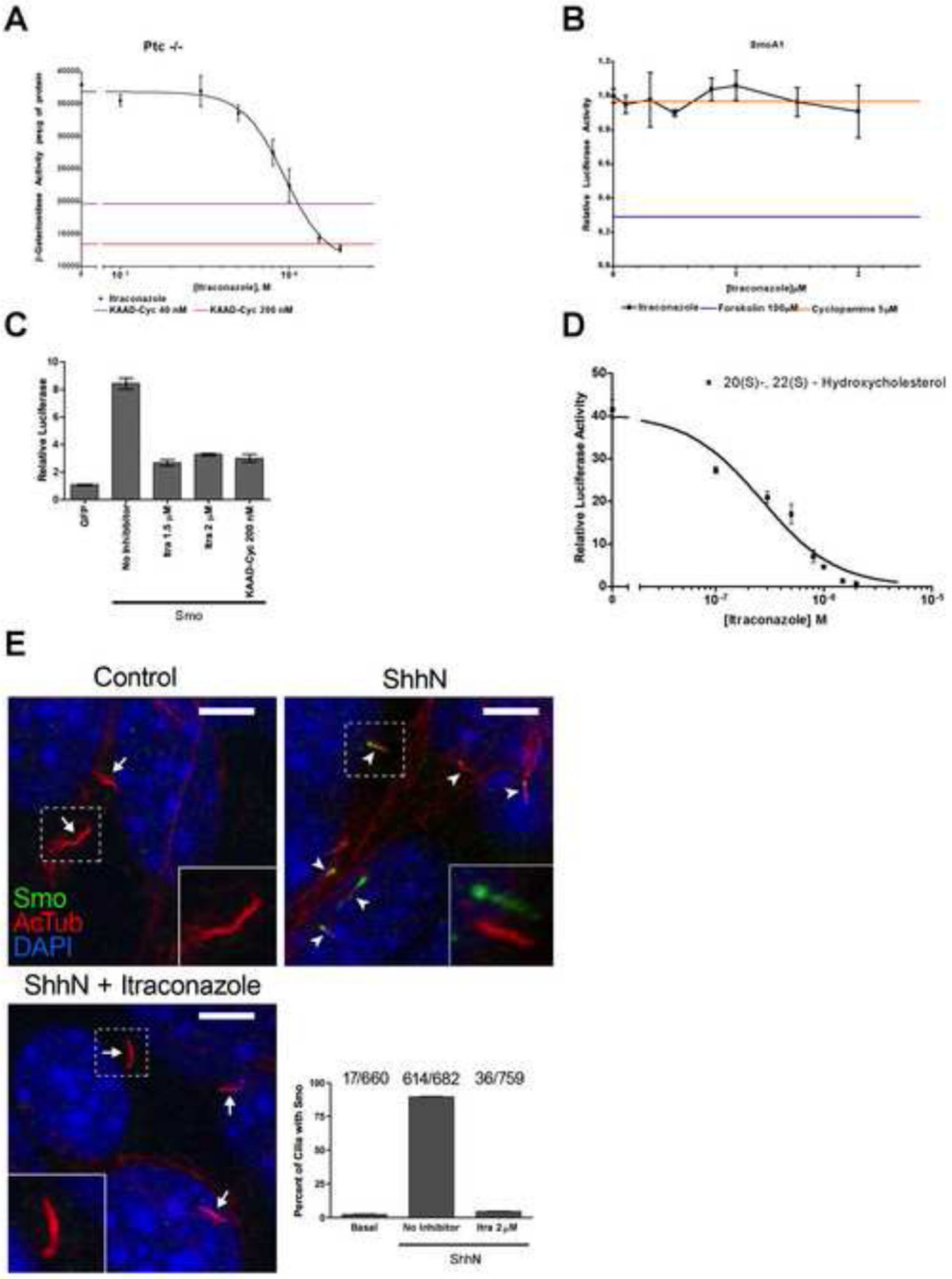

Figure 4. Mapping of itraconazole action within the Hh pathway

(A) Itraconazole inhibited constitutive Hh pathway activity in *Ptch*−/− cells, measured as expression of β-galactosidase activity from the *Ptch-lacZ* locus (Goodrich et al., 1997; Taipale et al., 2000). The levels of β-galactosidase activity from cells treated with KAAD-cyclopamine at 40 and 200 nM (2× and 10× IC_{50}) are shown as purple and red lines, respectively. (B) Shh-Light SmoA1 cells, stably expressing a constitutively active Smo mutant, were resistant to Hh pathway inhibition by itraconazole. Cyclopamine and forskolin (orange and blue lines, respectively) were used as negative and positive controls for the

inhibition of SmoA1. (C) Itraconazole and KAAD-cyclopamine both inhibited constitutive Hh pathway activation induced by transient overexpression of Smo in NIH-3T3 cells. (D) Itraconazole inhibited Hh pathway activity induced by the combined oxysterols, 20(S)-and 22(S)-hydroxycholesterol (5 μM each). All signaling assays were performed with Shh-Light2 cells in 0.5% serum media and data are shown as the mean of triplicates ± s.d. (E) Representative immunofluorescent images of NIHT-3T3 cells. Smo accumulated in primary cilia upon stimulation with ShhN (arrowheads). This accumulation was blocked by treatment with itraconazole. Insets show enlarged views of primary cilia in the dashed box, with Smo and acetylated tubulin channels offset. Arrows show primary cilia with no Smo accumulation. As seen in the histogram, the accumulation of Smo in ~90% of primary cilia of cells stimulated with ShhN, is reduced to ~5% in the additional presence of itraconazole. The number of primary cilia containing Smo over the total number of primary cilia are shown above each bar. Data are mean of 10 images ± s.d. The scale bar represents 5 μm.

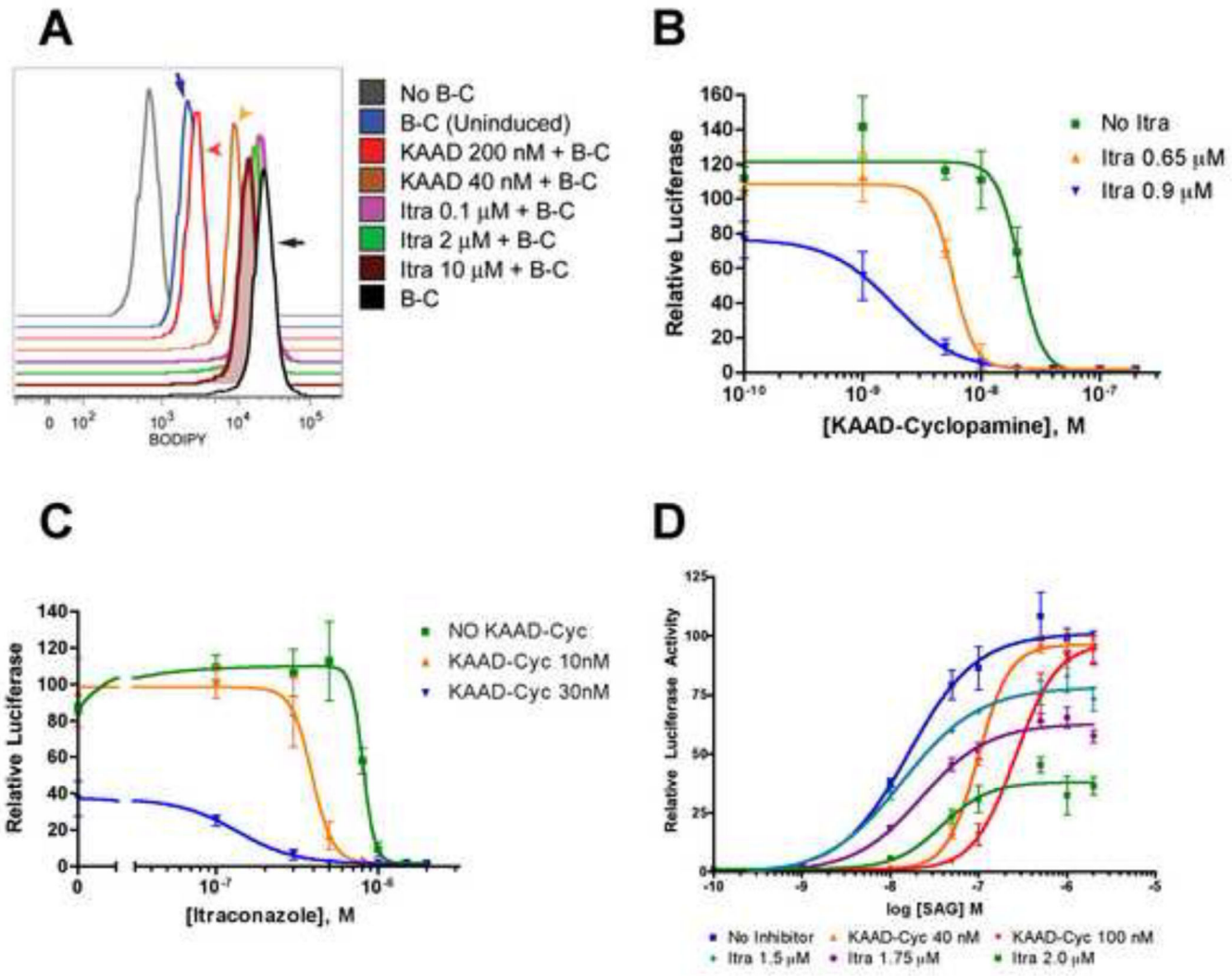

Figure 5. Itraconazole acts at a site distinct from the cyclopamine-binding site of Smo

(A) BODIPY-cyclopamine (B–C) bound to tetracycline-induced Smo in 293S cells as monitored by FACS. As negative controls, the grey tracing shows fluorescence of cells not treated with B–C and the blue tracing (blue arrow) shows uninduced cells treated with B–C; the black tracing (black arrow) represents maximal fluorescence of cells induced for Smo expression and treated with B–C. Itraconazole treatment (no arrows) at concentrations up to 12.5× IC_{50} (10 μM) did not effectively compete for B–C binding, whereas KAAD-cyclopamine at 2× IC_{50} and 10× IC_{50} (40 nM and 200 nM; tan and red arrowheads, respectively) caused significant decreases in fluorescence. (B, C) Synergistic action of itraconazole and KAAD-cyclopamine. In signaling assays performed with Shh-Light2 cells, the presence of itraconazole caused a downward shift in the IC_{50} of KAAD-cyclopamine (from 21 nM to 1.8 nM in the presence of 900 nM itraconazole; panel B and Table S2); KAAD-cyclopamine caused a downward shift in the IC_{50} of itraconazole (from 805 to 135 nM in the presence of 30 nM KAAD-cyclopamine; panel C and Table S3). (D) KAAD-cyclopamine is a competitive inhibitor of SAG, a known Hh pathway agonist, as shown by shifts of the SAG EC_{50} by ~5 and ~13 fold at 40 nM and 100 nM concentrations of KAAD-

cyclopamine. In contrast, itraconazole did not alter the SAG EC_{50} but decreased the maximal activity of SAG, thus acting as a noncompetitive inhibitor (see Table S4). All signaling assays were performed with Shh-Light2 cells in 0.5% serum media and data are mean of triplicates ± s.d.

See also Tables S2, S3, and S4.

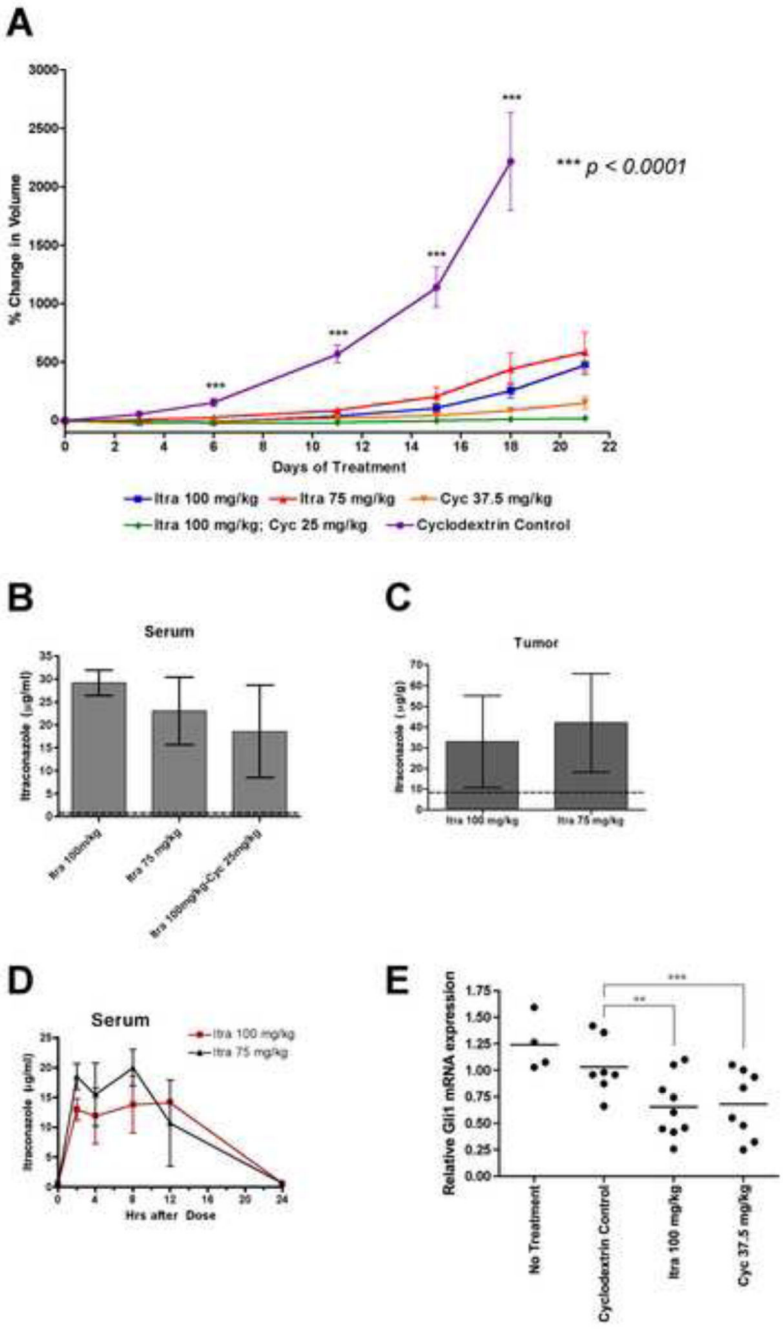

Figure 6. Itraconazole inhibits the growth of Hh-dependent medulloblastoma *in vivo*

(A) Itraconazole, either alone or in combination with cyclopamine, suppressed the growth of allografted medulloblastomas from a *Ptch+/−p53−/−* mouse, as compared to vehicle-treated tumors. Treatments were given twice per day by oral gavage. The number of tumors used in this experiment were: Cyclodextrin control $n = 8$, Itraconazole 100 mg/kg $n = 12$, Itraconazole 75 mg/kg $n = 10$, Cyclopamine 37.5 mg/kg $n = 10$, Itraconazole/cyclopamine $n = 10$. Data are expressed as mean percentage change in volume ± s.e.m. (B, C) Mean serum and tumor itraconazole levels obtained at the end of the allograft study in (A) are shown in

panels (B) and (C), respectively. The dashed lines represent the minimum detectable levels of the assay; vehicle controls were at or below these levels. (D) Pharmacokinetics of itraconazole levels in serum of athymic nude mice after one oral dose of itraconazole 100 mg/kg or 75 mg/kg. All itraconazole levels were obtained using the bioassay method (Clemons et al., 2002; Harvey et al., 1980; Hostetler et al., 1992; Rex et al., 1991). Data for itraconazole levels in panels (BD) are the mean of three samples ± s.d. (E) Hh pathway is decreased in allografted medulloblastoma tumors when treated with either itraconazole or cyclopamine as compared to cyclodextrin control treatment. Hh pathway was monitored by Gli1 mRNA levels. Gli1 mRNA levels of drug treatments were normalized to the mean of Gli1 mRNA levels of cyclodextrin control. Treatments were given twice per day for four days by oral gavage. ** $p = 0.0197$; *** $p = 0.0386$

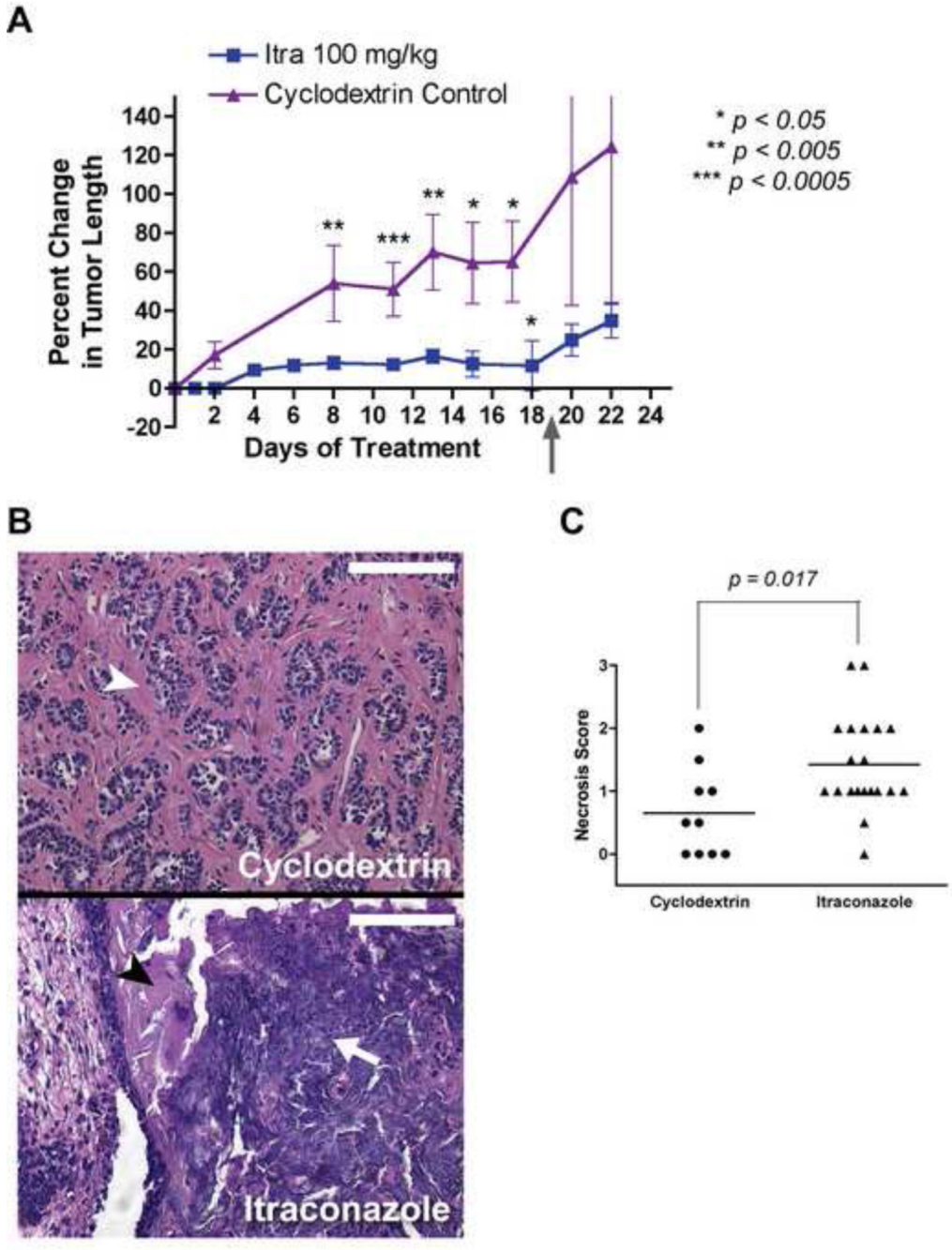

Figure 7. Itraconazole inhibits the growth of Hh-dependent basal cell carcinoma *in vivo*

(A) Compared to cyclodextrin vehicle treated tumors, itraconazole suppressed the growth of endogenous basal cell carcinomas from a *K-14CreER;Ptch+/−;p53 fl/fl* mouse. Treatments were given twice per day by oral gavage. Gray arrow indicates the day that itraconazole treatment was stopped. The number of tumors used in this experiment were: Cyclodextrin control $n = 10$, Itraconazole 100 mg/kg $n = 20$ until day 19 when itraconazole treatment was discontinued then $n = 6$ after some mice were euthanized and tumors dissected for further examination (see “Experimental Procedures”). For statistical analysis, pairwise comparisons

of treatment arms were made for corresponding day of treatment with the exception of cyclodextrin control day 17 being compared with itraconazole day 18. Data are expressed as mean percentage change in tumor length ± s.e.m. (B) Cyclodextrin control treated tumors showed nests of well organized tumor cells (arrowhead), whereas itraconazole-treated tumors showed greater evidence of necrosis as seen by destruction of organized nests of basophilic tumor cells and pyknosis (arrow) and destruction of eosinophilic stroma lining the BCC nests (black arrowhead). Images are H&E sections. The scale bar represents 100 μm. (C) From the tumor growth inhibition study, BCC tumors from itraconazole treated mice (including those that had itraconazole discontinued) show more evidence of necrosis than cyclodextrin control treated tumors as measured by necrosis score (see Experimental Procedures) with higher numbers indicating worsening necrosis.